January 2008

Cysteine Dioxygenase: The Importance of Key Residues and Insight into the Mechanism of the Metal Center

Jonathan H. Leung
University of Massachusetts Amherst

CYSTEINE DIOXYGENASE: THE IMPORTANCE OF KEY RESIDUES AND INSIGHT INTO THE MECHANISM OF THE METAL CENTER

A Thesis Presented

By

JONATHAN H. LEUNG

Submitted to the Graduate School of the
University of Massachusetts Amherst in partial fulfillment
Of the requirements for the degree of

MASTERS OF SCIENCE

May 2008

Molecular and Cellular Biology

CYSTEINE DIOXYGENASE: THE IMPORTANCE OF KEY RESIDUES AND INSIGHT INTO THE MECHANISM OF THE METAL CENTER

A Thesis Presented

By

JONATHAN H. LEUNG

Approved as to style and content by:

_____
Michael J. Maroney, Chair

_____
Alice Cheung, Member

_____
Michael Knapp, Member

_____
Patricia Wadsworth, MCB Director

ACKNOWLEDGMENTS

First, I would like to thank Michael J. Maroney, my advisor, for all the tireless help, patience, and support through out my time in his lab. I would also like to give special thanks to Sergio Chai for his guidance and setting a firm base for my lab work with CDO. Also thanks to Robert W. Herbst and David Kennedy for the aid with experiments and analysis. I would like to extend my gratitude to my committee members, Alice Cheung and Michael J. Knapp, for their comments and encouragement during the process.

I want to thank the American Chemical Society Petroleum Research Fund for funding this project and making this research possible. Also thanks to the University of Massachusetts Amherst for an education and further funding.

Also I would like to thank the whole Maroney lab for their support, help, and friendship. Also my friends and family that helped me get through the good and the bad times and kept me focused to get the job done.

ABSTRACT

CYSTEINE DIOXYGENASE: THE IMPORTANCE OF KEY RESIDUES AND INSIGHT INTO THE MECHANISM OF THE METAL CENTER

MAY 2008

JONATHAN H. LEUNG, B.S., UNIVERSITY OF MASSACHUSETTS AMHERST

M.S., UNIVERSITY OF MASSACHUSETTS AMHERST

Directed by: Professor Michael J. Maroney

Cysteine dioxygenase (CDO) is a non-heme iron enzyme that can be found in mammalian tissue. It is mainly localized in the liver but is also present in the brain, kidney, and adipose tissue. CDO converts cysteine to cysteine sulfinic acid, which is the first step in cysteine metabolism in the human body. CDO contains a novel cofactor located near the metal binding site that is present in another enzyme, galactose oxidase, where it is essential for redox function. This suggests that the linkage may play an important role in CDO as well. The cofactor consists of Y157 and C93. Mutation of the C93S causes a drop in activity to 57.1% and a mutation of the Y157F causes a drop to 8.1%. The metal center was studied using XAS revealing that the addition of cysteamine, an activator of CDO, changes the conformation of the binding site significantly. CDO differs from the rest of the cupin super family in that it does not contain a 2-his-1-carboxylate binding motif but rather the carboxylate is replaced with another histidine. A mutation of one of the binding residues, H140D, caused the enzyme to be non-active. Also the mechanism of the CDO was studied by conducting activity assays with various

inhibitors and activators that yielded contradicting results with previously published work.

TABLE OF CONTENTS

Page

LIST OF TABLES

LIST OF FIGURES

CHAPTER 1

CYSTEINE DIOXYGENASE

1.1 Introduction to Cysteine Dioxygenase

Cysteine dioxygenase (CDO) catalyzes the reaction of cysteine to cysteine sulfinic acid (CSA) by adding molecular oxygen to the thiol of cysteine (Figure 1.1). This reaction is the first step in the cysteine catabolic pathway. CDO plays a key role in maintaining intracellular sulfur concentrations. As such, CDO is mainly found in the liver, but appreciable amounts can also be found in the kidney, brain, lungs, and adipose tissue.[1,2,3] CDO has such a large impact on maintaining intracellular sulfur concentrations it can decrease steady state intracellular cysteine levels as well as glutathione levels.[4] High levels of cysteine are associated with the neurological diseases Alzheimer's and Parkinson's diseases.[5] Abnormal CDO activity and the accumulation of cysteine have been observed in patients suffering from the neurological disorder Hallervorden-Spatz syndrome.[6] CDO may directly affect the disease cystinosis. Cystinosis occurs when cysteine builds up and it begins to form disulfide bonds with each other forming the insoluble compound cystine.[7,8] CDO eliminates excess cysteine to avoid this condition.

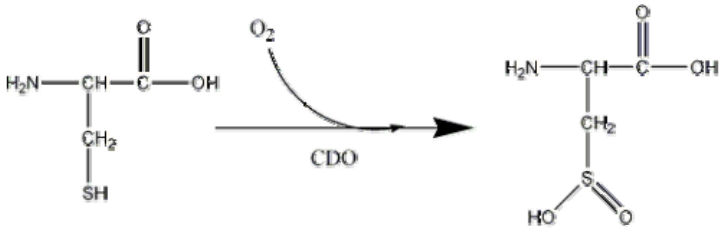

Figure 1.1. The conversion of cysteine to cysteine sulfinic (CSA) acid by CDO

After CSA is made it can undergo two major pathways, one ultimately resulting in taurine formation and the other creating pyruvate and sulfate. The taurine

pathway involves the decarboxylation of CSA by the enzyme cysteine sulfinate decarboxylate to form hypotaurine (2-aminoethane sulfonate).[9] Hypotaurine is then oxidized to taurine via a poorly understood pathway where enzymatic and non-enzymatic mechanisms may occur.[10] CSA can undergo a second pathways where transamination occurs to form β-sulfinylpyruvate, which spontaneously decomposes to sulfite and pyruvate.[11] Sulfite readily oxidizes to sulfate. Lack of cellular sulfate has also been associated with rheumatoid arthritis.[12]

CDO is a Fe(II) non-heme iron dioxygenase and contains significant sequence homology with other members of the cupin superfamily of proteins.[13] Members of this superfamily possess a ß-barrel with a jelly roll topology which can also be seen in the crystal structure (Figure 1.3).[13] Members of this family contain two conserved sequence motifs, $G(X)_5H(X)H(X)_{3,4}E(X)_6G$ and $G(X)_5P(X)G(X)_2H(X)_3N$ (Figure 1.2), derived from the superfamily archetype, germin.[14] The second sequence is less conserved than the first. The active site of these proteins are usually formed by a histidine and a carboxylate residue, either glutamate or aspartate, from the first motif and another histidine from the second motif forming the 2-his-1-carboxylate binding motif common among Cupin members. In CDO the carboxylate residue is replaced with another histidine forming a 3-histidine binding pocket.

```
-35  MGSSHHHHHH SSGLVPRGSH MLEGWTEETR PSPAG                  0
1    MERTELLKPRTLADLIRILHELFAGDEVNVEEVQAVLEAYESNPAEWALY    50
51   AKFDQYRYTRNLVDQGNGKFNLMILCWGEGHGSSIHDHTDSHCFLKLLQG   100
101  NLKETLFDWPDKKSNEMIKKSERTLRENQCAYINDSIGLHRVENVSHTEP   150
151  AVSLHLYSPPFDTCHAFDQRTGHKNKVTMTFHSKFGIRTPFTTSGSLENN   200
```

Figure 1.2. Amino acid sequence of recombinant CDO. Residues -35 to 0 represent the 6x histidine tag used for purification. Residues in green are conserved residues through out other CDOs in other organisms near the metal binding site. Residues in red represent the three metal binding histidines.

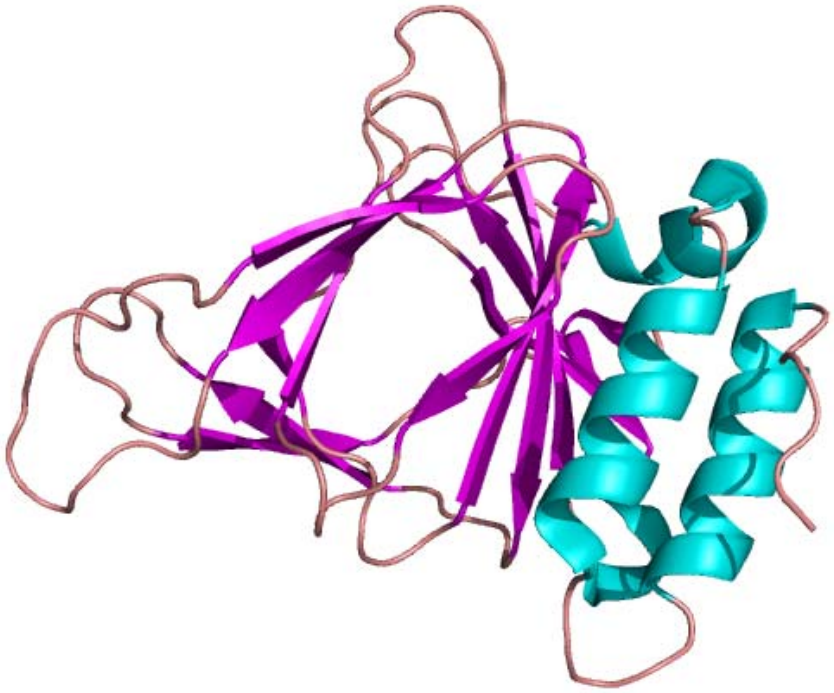

Figure 1.3. Crystal structure of rat CDO showing the typical jelly roll beta barrel. (PDB ID 2GH2)

Four crystal structures of CDO have been resolved, three eukaryotic and one prokaryotic. These proteins came from mouse, rat, human, and *Ralstonia eutropha* (Figure 1.4).[15,16,17,18] All the crystal structures show different binding geometries with different bound molecules but all contain the 3-histidine metal binding site. The mouse protein had nickel bound to the active site and was octahedral with the three histidines arranged as a facial triad with aqua molecules opposing them.[15] Then the rat structure was modeled with an iron bound to one aqua ligand and the three histidines in a tetrahedral formation.[16] The other two structures were modeled with iron and found to be 5-coordinate with a cysteine or two aqua molecules in the human and bacterial enzymes respectively.[17,18]

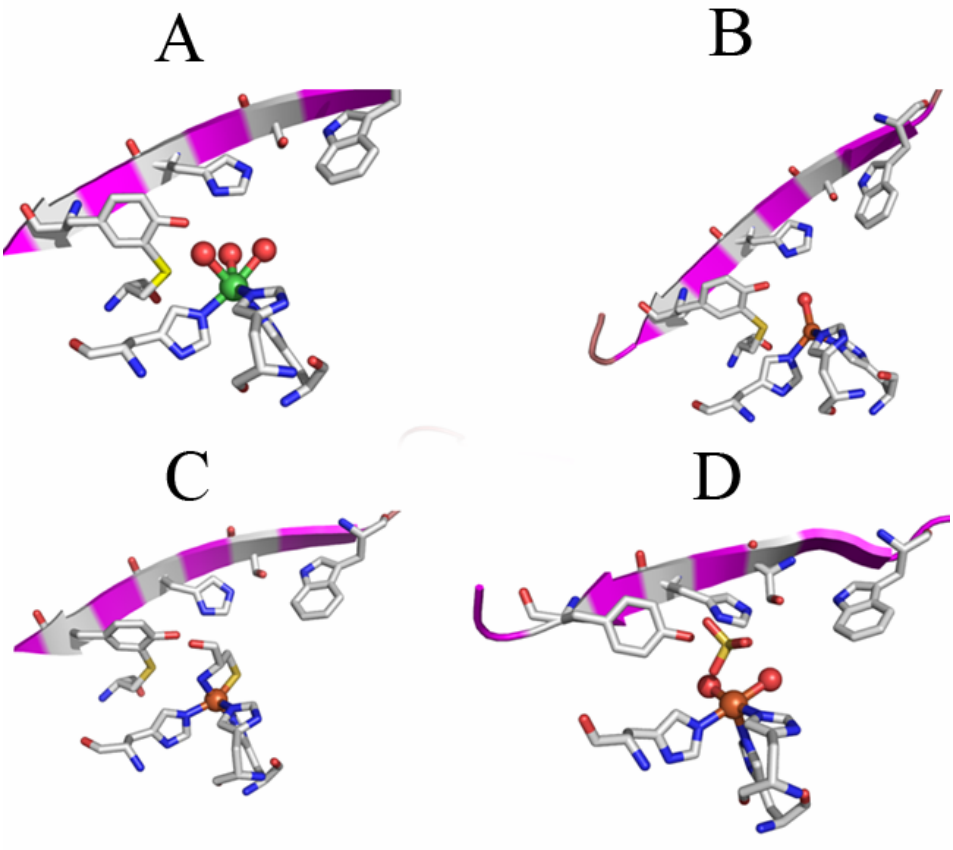

Figure 1.4. Metal binding sites of the four solved CDO crystal structures. (A) Mouse with Ni(II) bound (2ATF). (B) Rat with Fe(III) bound (2B5H). (C) Human with Fe(II) bound and cysteine in the binding site (2IC1). (D) The bacterial *Ralstonia Eutropha* with Fe(III) bound with a sulfate in the binding site (2GM6).

The prokaryotic CDO also contains another unique feature from the other crystal structures. All but the bacterial structure reveals a novel cysteinyltyrosine cofactor. In the prokaryotic CDO the bridging cysteine is replaced by a glycine, disrupting the linkage.[18] This linkage is well characterized in only one other enzyme, galactose oxidase. In galactose oxidase the linkage is required for enzyme functionality where it serves as an internal redox cofactor.[19] Using site directed mutagenesis it was possible to convert cysteine-93 and tyrosine-157 to a serine and

phenylalanine respectively. With these mutations it is possible to study the importance of these residues and if the residues or the linkage between them are required for catalysis.

Another novel feature of CDO is the 3-histidine metal binding site only shared by a few other members of the cupin superfamily such as diketone dioxygenase.[20] The more common 2-his-1-carboxyl binding motif is found amongst most of the Cupin superfamily. This motif is found to bind many more metals than iron while still yielding functional enzyme where as the 3-histidine motif does bind many various metals,[20] but only when Fe(II) is bound to the active site is functional enzyme is yielded. Again, using site-directed mutagenesis the 2-his-1-carboxyl motif will be restored and its affects on CDO will be assessed.

More insight into the mechanism and binding pocket of CDO is found by using x-ray spectroscopic techniques. Using extended x-ray absorption fine structure (EXAFS) it will be possible to see what geometry around the metal center is formed in unbound substrate, bound substrate, and bound with the activator cysteamine. It will give information about how the substrate binds whether it is by the carboxyl, amino, thiol or if the substrate is bound directly to the iron at all. The ligand distances around the iron will be found and used to determine possible functions of the various residues located around the metal.

1.2 Experimental

1.2.1 Over Expression in Escherichia Coli

Recombinant rat CDO-ORF was previously subcloned into the vector pET-14b and transferred into the *E. Coli* strain BL21(D3)pLysS. The cells are grown in

LB broth at 22 ^{o}C for 8 hours. At this time the expression of CDO is induced by addition of IPTG and ferrous ammonium sulfate to a final concentration of 200 μM each. Then the cells were grown for an additional 16 hours at 22 ^{o}C.

Cells were harvested by centrifugation and resuspended in 50 mM Phosphate, pH 8.0, also containing 300mM sodium chloride buffer and 10 mM imidazole. This suspension is kept frozen in a –20 ^{o}C freezer for future analysis. The cells are lysed by thawing in the presence of phenylmethylsulfonyl fluoride (PMSF) and Benzonuclease. SDS-PAGE using the Laemmli method is used to confirm the expression of CDO.[21]

1.2.2 Purification of Recombinant CDO

The cell lysis is centrifuged to pellet the solid cell debris. The recombinant CDO contains an extra 35 amino acid his-tag sequence attached to the N-terminal end of the protein. The supernatant was ran over a nickel-nitrilotriacetic acid (NTA) column and the nickel will bind the his-tag of CDO purifying it from other impurities. The bound protein is washed with 1.5 L of 50 mM phosphate buffer, pH 8.0, containing 300mM sodium chloride and 30mM imidazole. After washing, the protein is eluted from the column with a 50mM phosphate buffer, pH 8.0, containing 300mM sodium chloride and 300mM imidazole. SDS-PAGE with the Laemmli method is used again to confirm that pure protein was eluted from column (Figure 1.5).[21]

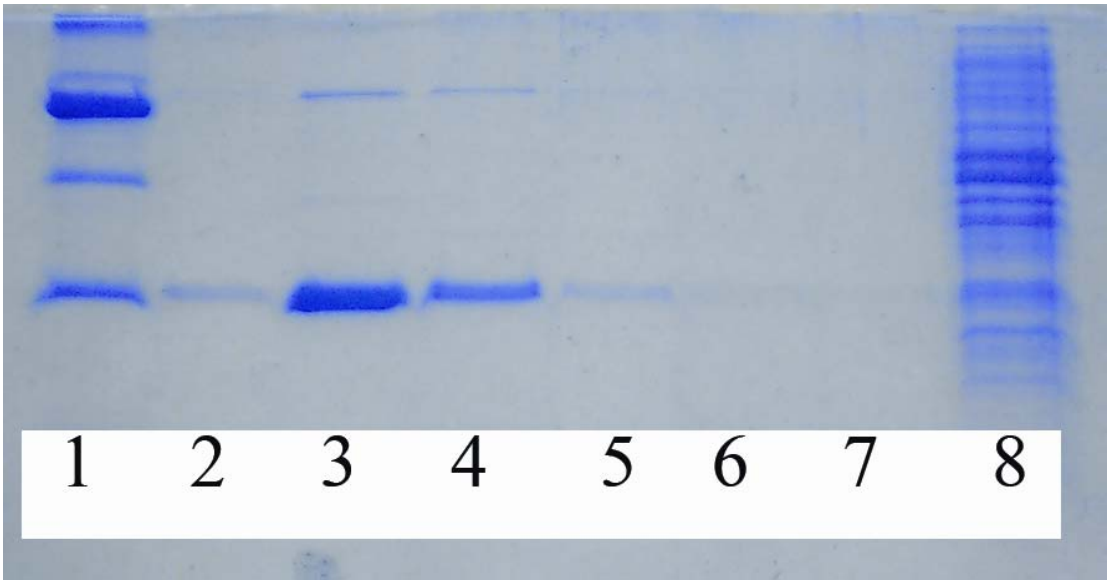

Figure 1.5. SDS-PAGE gel after CDO purification. (Lane 1) Marker. (Lanes 2-7) elutions 1-6 from NTA column. (Lane 8) Cell lysis with CDO removed. The last marker represents 24 kDa.

The elution is then concentrated with 10,000 Da cutoff 5 mL spin concentrators to a final protein concentration of approximately 100 μM and then buffer exchanged into 50 mM phosphate or HEPES buffer, pH 7.5 containing 100mM sodium chloride. The iron content of the sample is determined by ICP-OES in the same buffer and the final concentration of the sample is determined with bicinchonic acid (BCA) protein assay (Pierce).

1.2.3 Activity Assay

A water bath is preheated to 37^{o}C. 1.5 mL centrifuge tubes (epi-tubes) were filled with varying substances depending on the test being performed. A standard test with CDO saturated for V_{max} determination includes 50 μL of CDO and 950 μL of 30 mM cysteine for final concentrations of 4.5 μM and 23.2 mM respectively. The tubes were incubated in the water bath for 3.5-5 hours. After this, the reactions were stopped by the addition of 20 μL of heptafluorobutyric acid (HFBA) to each epi-tube.

The HFBA causes the CDO to precipitate out of solution. The CDO was pelleted with centrifugation and the supernatant was aliquoted into a separate high performance liquid chromatography (HPLC) vial. Analyses of the samples were done in two ways, HPLC and induced coupled plasma with optical emission spectra (ICP-OES).[22]

1.2.4 Activity Analysis of CDO

1.2.4.1 Use of High Performance Liquid Chromatograph (HPLC)

The mobile phase that was used is a 99.4:0.6 (v/v) ratio of water:methanol solution containing 3% HFBA. Flow conditions were 50 µL of sample injected at a flow rate of 0.8 mL/min for 20 minutes. Two Agilent C_{18} columns were used for separation. Detection of substances were done by the use of a ultra-violet light detector at the wavelengths 215nm and 230nm (Figure 1.6).[22]

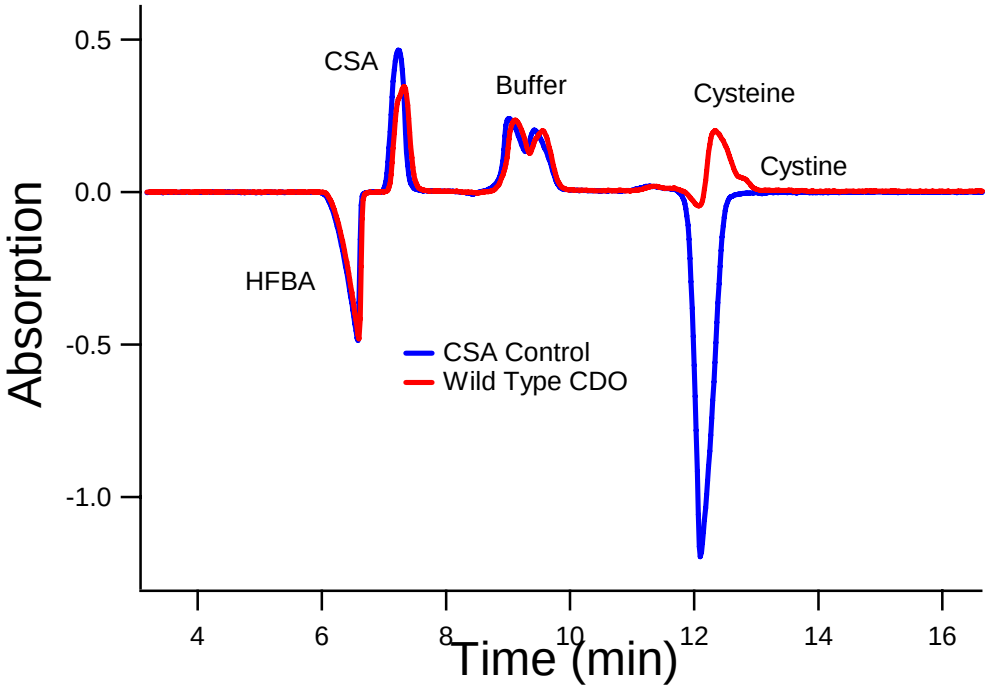

Figure 1.6. Activity assay chromatogram from HPLC. Absorption is at 215 nm.

1.2.4.2 Use of Induced coupled plasma with optical emissions spectra (ICP-OES)

The same mobile phase for ICP-OES is used as in the HPLC analysis. Flow rate on the ICP-OES was set at 1 mL/min and was ran for 10 minutes. Only one Agilent C_{18} column is needed for separation. The detector was set for a sulfur emission line at a wavelength of 181.975nm (Figure 1.7).

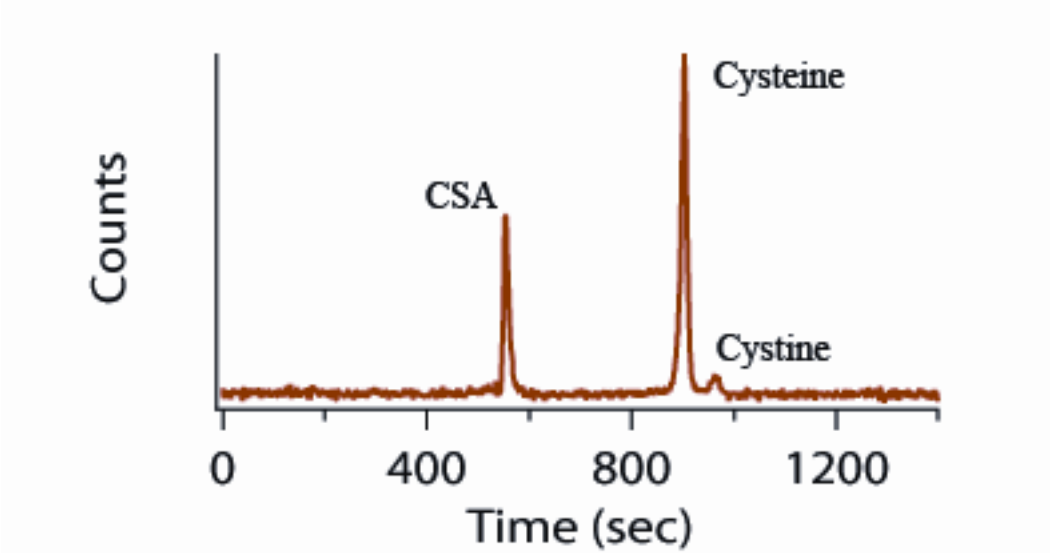

Figure 1.7. Activity Assay chromatogram from ICP-OES.

1.2.5 Cleavage of His-tag from Recombinant CDO

Thrombin attached to agarose beads were washed three times with a 1x cleavage buffer (50 mM Tris-HCl, pH 8.0, 10 mM $CaCl_2$) by using centrifugation and then decanting the supernatant. The CDO was buffer exchanged into 1x cleavage buffer. 1 mg of CDO was added to an epi-tube along with 100 µL of 10x cleavage buffer. This solution was diluted to 1 mL with DI water. The solution was placed on a rotating platform to flip and agitate the solution for 24 hrs. The cleaved protein was retrieved by the same method as the wash except the supernatant is decanted into a

separate epi-tube and stored at 4 ^{o}C. Confirmation of cleavage is done by SDS-PAGE looking for a band at 23 kDa.

1.3 Results and Discussion

The expression of the recombinant enzyme was confirmed by SDS-PAGE. The SDS-PAGE clearly shows a thick band slightly above the 24 kDa marker. This band represents CDO with a histidine tag. The elution of CDO from the Ni-NTA column is done in six 10 mL aliquots. Most of the CDO is concentrated in the second aliquot, but reasonable amounts are distributed among the first, third, and fourth as well. (Figure 1.5) The purpose of the fifth and sixth aliquots is to make sure all CDO has been eluted. The gel also detects a high molecular weight peptide. It is unclear what this band is. The protein is still quite pure because the band is faint and does not represent much protein. It is possible that this peptide could represent the 68kDa sized CDO protein that was found by Waring and co-workers. This protein found by Waring did not dissociate under reducing conditions with SDS or with boiling.[23,24]

The eluted protein is concentrated using 10 kDa spin concentrators. Then it is buffer exchanged. At first a phosphate buffer pH 7.5 containing 100mM sodium chloride was used because it was most stable in that buffer but then it was found to be also stable in HEPES buffer pH 7.5 containing 100mM sodium chloride, so HEPES buffer was then used. HEPES buffer was chosen over phosphate buffer because of the convenience for metalation and thrombin cleavage. The samples of protein come out to an approximate volume of 2 mL and concentration of 100 μM per liter of culture. This varies from purification to purification. The sample is tested for activity, which can be seen in the chromatograms above (Figure 1.6 and 1.7). Iron content of the

CDO samples have an average of 10%, but have been as low as 6%. Recently it was possible to incorporate 26% iron into the enzyme using a slightly modified metalation scheme by ripping out other metals by chelation with EDTA and adding iron ammonium sulfate to the final purified product under anaerobic conditions

When enzyme is confirmed for purity and activity it may be cleaved to remove the histidine-tag. The purpose of this is to increase maximum concentration that CDO can achieve without precipitating out of solution. Increased concentrations are needed for several of the following experiments described later such as X-ray Absorption Spectra (XAS). Also thrombin cleavage is needed to prepare enzyme for crystallization because the native enzyme is needed.

1.4 References

(1) Hirschberger LL, Daval S, Stover PJ, Stipanuk MH. Murine cysteine dioxygenase gene: structural organization, tissue-specific expression and promoter identification. *Gene* **2001**, 277, 153-161.

(2) Stipanuk MH, Londono MP, Lee JI, Hu M, Yu AF. Enzymes and metabolites of cysteine metabolism in nonhepatic tissues of rats show little response to changes in dietary protein or sulfur amino acid levels. *J. Nutr.* **2002**, 132, 3369-3378.

(3) Tsuboyama N, Hosokawa Y, Totani M, Oka J, Matsumoto A, et al. Structural organization and tissue-specific expression of the gene encoding rat cysteine dioxygenase. *Gene* **1996**, 181, 161-165

(4) Dominy JE Jr., Hwang J, Stipanuk MH. Overexpression of cysteine dioxygenase reduces intracellular cysteine and glutathione pools in HepG2/C3A cells. *Am J Physiol. Endocrinol. Metab.* **2007**, 293(1), E62-E69.

(5) Parsons RB, Waring RH, Ramsden DB, Williams AC. In vitro effect of the cysteine metabolites homocysteic acid, homocysteine and cysteic acid upon human neuronal cell lines. *Neurotoxicology* **1998**, 19, 599-603.

(6) Perry TL, Norman MG, Yong VW, Whiting S, Crichton JU, Hansen S, Kish SJ. Hallervorden-Spatz disease – cysteine accumulation and cystine dioxygenase deficiency in *Globus pallidus*. *Annals of Neurology* **1985**, 18, 482-489

(7) Kalatzis V, Cherqui S, Antignac C, Gasnier B. Cystinosin, the protein defective in cystinosis, is a H+-driven lysosomal cystine transporter. *EMBO Journal* **2001**, 20, 5940-5949.

(8) Kalatzis V, Antignac C. Cystinosis: from gene to disease. *Nephrology Dialysis Transplantation* **2002**, 17, 1883-1886.

(9) Guionrain MC, Portemer C, Chatagner F. Rat-liver cysteine sulfinate decarboxylase – purification, new appraisal of molecular-weight and determination of catalytic properties. *Biochimica Et Biophysica Acta* **1975**, 384, 265-276.

(10) Griffith OW. *Mammalian sulfur amino acid metabolism*. Academic Press: Orlando, Florida, **1987**, 143

(11) Singer TP, Kearny EB. Intermediary metabolism of L-cysteinesulfinic acid in animal tissues. *Archives of Biochemistry and Biophysics* **1956**, 61, 397-409.

(12) Emery P, Bradley H, Gough A, Arthur V, Jubb R, Waring R. Increased prevelance of poor sulfoxidation in patients with rheumatoid-arthritis – effects of changes in the acute phase response and 2nd-line drug-treatment. *Annals of the Rheumatic Diseases* **1992**, 51, 318-320.

(13) Gough J, Karplus K, Hughey R, Chothia C. Assignment of homology to genome sequences using a library of hidden Markov models that represent all proteins of known structure. *J. Mol. Biol.* **2001**, 313, 903-919.

(14) Dunwell JM, Culham A, Carter CE, Sosa-Aguirre CR and Goodenough PW. Evolution of functional diversity in the cupin superfamily. *Trends Biochem. Sci.* **2001**, 26, 740-746

(15) McCoy JG, Bailey LJ, Bitto E, Bingman CA, Aceti DJ, Fox BG, Phillips GN. Structure and mechanism of mouse cysteine dioxygenase. *P. Natl. Acad. Sci. USA*. **2006**, 103, 3084-3089.

(16) Simmons CR, Liu Q, Huang Q, Hao Q, Begley TP, Karplus PA, Stipanuk MH. *J. Biol. Chem.* **2006**, 281, 18723-18733.

(17) Ye S, Wu X, Wei L, Tang D, Sun P, Bartlam M, Rao Z. Insight into the mechanism of human cysteine dioxygenase key roles of the thioether-bonded-tyrosine-cysteine cofactor. *J. Biol. Chem.* **2007**, 282(5), 3391-3402.

(18) Simmons CR, Karplus PA, Stipanuk MH. 1.5 A Resolution R. Norvegicus Cysteine Dioxygenase Structure Crystallized in the Presence of Cysteine. Unpublished but PDB deposited.

(19) Firbank SJ, Rogers MS, Wilmot CM, Dooley DM, Halcrow MA, Knowles PF, McPherson MJ, Phillips SEV. Crystal structure of the precursor of galactose oxidase: An unusual self-processing enzyme. *PNAS***. 2001**, 98(23), 12932-12937.

(20) Straganz GD, Nidetzky B. Variations of the 2-his-1-carboxylate them in mononuclear non-heme Fe(II) oxygenases. *Chem. Biochem.* **2006**, 7, 1536-1548.

(21) Laemmli UK. Cleavage of structural proteins during the assembly of the head of bacteriophage T4. *Nature*. **1970**, 227(5259), 680-685.

(22) Chai SC, Jerkins AA, Banik JJ, Shalev I, Pinkham JL, Uden PC, Maroney MJ. Heterologous expression, purification, and characterization of recombinant rat cysteine dioxygenase. *J. Biol. Chem.* **2005**, 280(11), 9865-9869.

(23) Parsons RB, Ramsden DB, Waring RH, Barber PC, Williams AC. Hepatic localisation of rat cysteine dioxygenase. *J. Hepatol*. **1998**, 29, 595-602.

(24) Wilkinson LJ, Waring RH. Cysteine dioxygenase: modulation of expression in human cell lines by cytokines and control of sulphate production. *Toxicol. In Vitro*. **2002**, 16, 481-483.

CHAPTER 2

MUTATION OF THE CYSTEINLYTYROSINE COFACTOR IN CYSTEINE DIOXYGENASE

2.1 Introduction

One class of enzyme cofactors arises from covalent modifications of amino acid side chains. A common example of this is a disulfide bond between two cysteines due to the spontaneous oxidation of the thiol in the presence of oxygen. There are other examples of covalent cofactors but are usually rare. These include the cysteinyltyrosine thioether bond in galactose oxidase, tyrosine-histidine bond in cytochrome C oxidase, tryptophan-tryptophan bond in methylamine dehydrogenase, histidine-cysteine bridge in catechol oxidase, and 2,4,5-trihydroxyphenylalanine quinine in copper amine oxidase.[1,2,3,4,5] All of the cofactors in these enzymes serve as redox active amino acids.[6]

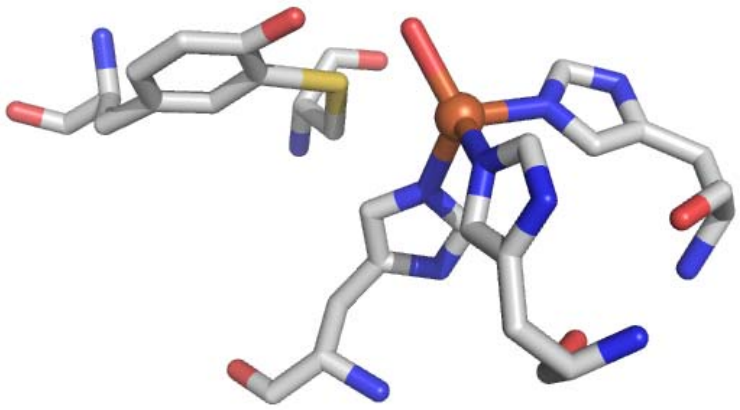

Figure 2.1. The metal binding site with iron bound, but clearly showing the cysteinyltyrosine cofactor on the upper left.

As mentioned before, in section 1.1, four crystal structures have been solved and three of the four contain a cysteinyltyrosine cofactor (Figure 2.1), this puts CDO into a short list of enzymes that contain cofactors.[7,8,9] This thioether cofactor is very rare and is only well characterized in one other enzyme, galactose oxidase (Figure 2.2).[10] It is thought it is also present in glyoxal oxidase, but is only characterized through resonance Raman spectroscopy and optical absorption spectra.[11] In galactose oxidase, the cofactor is redox active and a copper ligand.[10] The bridging bond is a post-translational modification. It has been shown that if this modification does not occur, the enzyme is non-functional.[10]

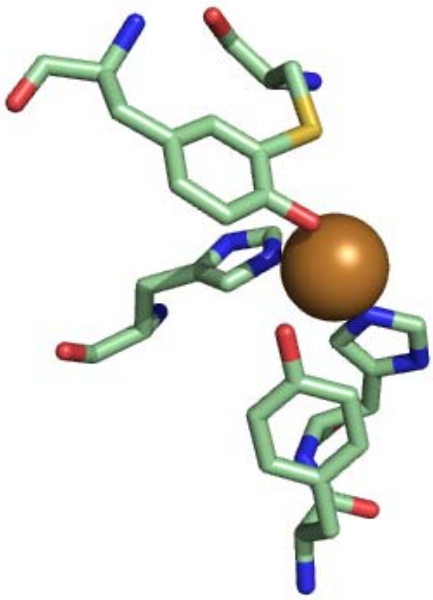

Figure 2.2 Metal Binding site of galactose oxidase. The copper is bound by Tyr272, Tyr495, His496, and His581. Tyr272 is also involved in a thioether bond with Cys228.

It is possible that the cofactor in CDO serves a purpose similar to that of galactose oxidase. It is believed that the cofactor most likely does not serve as a reducing agent because the cysteinyltyrosine does not exist in the bacterial CDO

crystal structure, where the cysteine is replaced by a glycine.[12] Thus, despite the lack of the cofactor, the enzyme is able to function as a dioxygenase. Instead the cysteinyltyrosine may serve as an intermediate stabilizer during the reaction mechanism through hydrogen bonding. The following mutagenesis experiments were performed to determine the function of the cofactor and help characterize CDO's mechanism and unique structure.

2.2 Experimental

2.2.1 Mutation of the Cysteinyltyrosine Cofactor

Two mutations were done for the characterization of cysteinlytyrosine. These mutations were C93S and Y157F. They were made using site-directed mutagenesis. The DNA plasmid, pET-14b containing the recombinant rat CDO-ORF, was isolated from *E. Coli* BL21(D3)pLysS cells that contained it using a miniprep assay (Qiagen). Reverse transcription polymerase chain reaction was performed using the respective primers for each mutation (Table 2.1). Confirmation of the mutation was performed by DNA sequencing obtained at Keck laboratory in Yale. When the mutation was confirmed, the mutated plasmid was transformed into the super-competent cell line, Nova Blue, and plated on LB containing ampicillin.

Table 2.1. Primer sequence for the cysteinyltyrosine cofactor mutations

Mutation	Forward Primer	Reverse Primer
C93S	3'-cac acg gac tcc cac tcc ttt ttg aag ctg ctg-5'	3'-cag cag ctt caa aaa gga gtg gga gtc cgt gtg-5'
Y157F	3'-gtg agc ctt cac ttg ttc agt cca cct ttc gat ac-5'	3'-gt atc gaa agg tgg act gaa caa gtg aag gct cac-5'

A culture of Nova Blue cells were grown in LB broth containing ampicillin overnight and subsequently pelleted and miniprepped. The DNA from the miniprep was transformed into BL21(D3)pLysS cells and plated. Finally overnight cultures

were grown in LB broth containing ampicillin and chloramphenicol and then samples were flash frozen in cryogenic tubes with liquid nitrogen and stored in a -80^{o}C freezer as a cell stock.

2.2.2 Michaelis Menten Kinetics of the Mutants

Assay conditions similar to those of the standard activity assay described in section 1.2.3 were used to assay the mutant enzymes. Eight reactions were performed per mutant with the cysteine concentrations varying from 0-23mM. Assays are analyzed as described above in section 1.2.4 and the results are plotted with cysteine versus enzyme activity.

2.3 Results

Two mutations were made to test the importance of the cysteinyltyrosine cofactor, C93S and Y157F. Both of these mutations disrupt the covalent bond and were chosen because the residues best replace the existing residues in terms of size and chemistry. Figure 2.3 shows the results plotted as a Michaelis Menten graph, which then can be seen summarized in table 2.2. The activity is normalized to iron content because enzyme is only active when iron is incorporated in the active site. Since CDO only binds about 10% and that number varies from samples to sample, each of the activities need to be normalized to get the true activity.

Table 2.2. Table of activities for cysteinyltyrosine mutants normalized to iron content.

Sample	Activity (mol CSA/min/mol Fe)	Percent Activity (compared to wild type)	K_m (mM)	k_{cat}/K_m (M^{-1} s^{-1})
Wild Type	41.8±7.3	100%	1.8±0.2	1.3E3±0.5
C93S	23.9±4.5	57.2%	1.6±0.2	7.8E2±0.5
Y157F	3.4±0.3	8.1%	.17±0.01	1.0E3±0.3

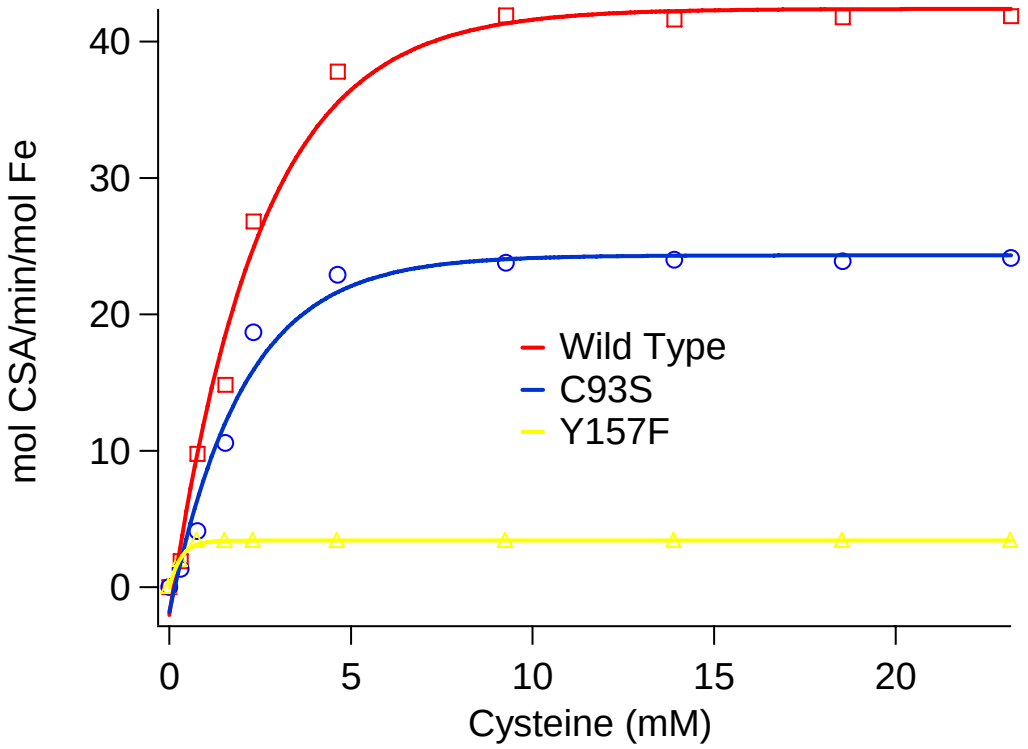

Figure 2.3. Michaelis Menten graph of cysteinyltyrosine mutants.

2.4 Discussion

The results show that the cysteinyltyrosine is not required for activity in context to its role in galactose oxidase. In galactose oxidase if the cofactor is disrupted in any way then the enzyme is no longer active.[10] In CDO, the elimination of the cofactor in the C93S mutant caused a decrease in activity of 42.8%. Also Y157F, which changed the residue closest to the metal center, still had 8.1% activity. Although this is a significant drop in activity, it proves that the cofactor is not required for activity. Instead each of the residues involved serve different purposes.

The large drop in activity due to the loss of the tyrosine may suggest that it is involved in forming the enzyme substrate complex. The hydroxyl group may serve as a hydrogen bond donor or proton donor to help stabilize the intermediates. The

cysteine has a less important role. The cofactor provided by the cysteine appears to be merely a stabilizing bridge for the more important tyrosine. When the cysteine is removed, the cofactor breaks and the tyrosine is less rigid. Less rigidity means that the tyrosine can move and "flop" around causing it to adopt conformations that some of the time don't stabilize the intermediates, thus the reaction goes slower. The function of the cysteine would then be to hold the tyrosine in place. This forces the hydroxyl group to point directly to a pocket in the metal center where the substrate may bind.

The less crucial role of the cysteine explains why it doesn't exist in the bacterial enzyme but the tyrosine does. The reason for this evolutionary difference in enzyme structure maybe because full activity of the enzyme is not needed. Having the fully functional enzyme as it exists in mammals may be detrimental to the bacteria because too much cysteine would be converted to CSA leaving too little for other functions such as other protein expression. For the bacterial enzyme from *Ralstonia eurtropha*, the tyrosine by it self has enough activity for its function.

Overall the characterization of the cysteinyltyrosine cofactor gives some insight into the mechanism of the reaction and more information on how the oxygenases of the cupin superfamily function.

2.5 References

(1) Whittaker MM, Duncan WR, Whittaker JW. Synthesis, structure, and properties of a model of galactose oxidase. *Inorganic Chem.* **1996**, 35, 382-386.

(2) Ostermeier C, Harrenga A, Ermler U, Michel H. Structure at 2.7 Å resolution of the *Paracoccus denitrificans* two-subunit cytochrome *c* oxidase complexed with an antibody Fv fragment. *Proc. Natl. Acad. Sci. USA*, **1997**, 94, 10547-10553.

(3) Chen LY, Doi N, Durley RCE, Chistoserdov AY, Lidstrom ME, Davidson VL, Mathews FS. Refined crystal structure of methylamine dehydrogenase from *Paracoccus denitrificans* at 1.75 Å resolution. *J. Mol. Biol.* **1998**, 276, 131-149.

(4) Klabunde T, Eicken C, Sacchettini JC, Krebs B. Crystal structure of a plant catechol oxidase containing a dicopper center. *Nat. Struct. Biol.* **1998**, 5, 1084-1090.

(5) Janes SM, Mu D, Wemmer D, Smith AJ, Kaur S, Maltby D, Burlingame AL, Klinman JP. A new redox cofactor in eukaryotic enzymes: 6-hydroxydopa at the active site of bovine serum amine oxidase. *Science*. **1990**, 248, 981-987.

(6) Okeley NM, Van der Donk WA. Novel cofactors via post-translational modifications of enzyme active sites. *Chem. Biol.* **7,** R159-R171.

(7) McCoy JG, Bailey LJ, Bitto E, Bingman CA, Aceti DJ, Fox BG, Phillips GN. Structure and mechanism of mouse cysteine dioxygenase. *P. Natl. Acad. Sci. USA*. **2006**, 103, 3084-3089.

(8) Simmons CR, Liu Q, Huang Q, Hao Q, Begley TP, Karplus PA, Stipanuk MH. *J. Biol. Chem.* **2006**, 281, 18723-18733.

(9) Ye S, Wu X, Wei L, Tang D, Sun P, Bartlam M, Rao Z. Insight into the mechanism of human cysteine dioxygenase key roles of the thioether-bonded-tyrosine-cysteine cofactor. *J. Biol. Chem.* **2007**, 282(5), 3391-3402.

(10) Firbank SJ, Rogers MS, Wilmot CM, Dooley DM, Halcrow MA, Knowles PF, McPherson MJ, Phillips SEV. Crystal structure of the precursor of galactose oxidase: An unusual self-processing enzyme. *PNAS***. 2001**, 98(23), 12932-12937.

(11) Whittaker MM, Kerstern PJ, Nakamura N, Sanders-Loehr J, Schweizer ES, Whittaker JW. Crystal structure of the precursor of galactose oxidase: An unusual self-processing enzyme. *J. Biol. Chem.* **271**, 681-687.

(12) Simmons CR, Karplus PA, Stipanuk MH. 1.5 A Resolution R. Norvegicus Cysteine Dioxygenase Structure Crystallized in the Presence of Cysteine. Unpublished but PDB deposited.

CHAPTER 3

PROBING THE 2-HISTIDINE-1-CARBOXYLATE MOTIF OF THE CUPIN SUPERFAMILY

3.1 Introduction

As mentioned above, the cupin super family typically contains a 2-histidine-1-carboxylate motif, but there are variations to this.[1] For instance, Quercetin Dioxygenase (QDO) contains a 3-histidine-1-carboxlyate binding pocket.[2] Most importantly to this thesis is the 3-histidine motif of CDO. It has been shown that most non-heme iron oxygenases of the 2-histidine-1-carboxylate motif also require α-ketoglutarate as a co-substrate.[3] α-ketoglutarate acts as a co-substrate and accepts one of the oxygen atoms and decomposes to carbon dioxide and succinate.[3] This is coupled with the oxidation of the main substrate.[3] These α-ketoglutarate dependent enzymes catalyze a diverse amount of reactions like side-chain modifications, DNA/RNA repair, metabolism, and degredation of many compounds.[3]

The source of power for the catalysis of these reactions is believed to come from oxygen activation.[4] Here it is hoped to elucidate the mechanism by which CDO catalyzes its reaction. CDO is not a α-ketoglutarate dependent oxygenase and it contains a unique binding pocket. The differences in CDO compared to the other members of the cupin superfamily suggest it reacts differently. This means there are no significant clues into how the mechanism of CDO works. Also the sulfur on the cysteine readily oxidizes; this suggests that the sulfur does not need a strong oxidizing agent for the reaction to occur.

The following experiments hope to elucidate some of the mechanism by mutating one of the histidines in the binding pocket to a carboxylic amino acid. The carboxyl group of the amino acid should provide the iron atom with more oxygen activating potential. If CDO undergoes oxygen activation as a part of its mechanism, then CDO should still be able to catalyze its reaction.

3.2 Experimental

3.2.1 Creating the 2-Histidine-1-Carboxylate motif through mutation

Site-directed mutagenesis is performed using the same protocol as described in chapter 3 when creating the cysteinyltyrosine mutations. In the cysteinyltyrosine mutants it was possible to use the mixture of pLysS and pET-14b vectors. The pET-14b vector contains the CDO-ORF and the pLysS vector comes in all the BL21(D3)pLysS cells. In the case of H140D the RT-PCR did not work with the mixture, so the pET-14b vector which contained the CDO-ORF had to be purified alone.

To do this DNA purification, both plasmids were isolated using the "DNA miniprep kit" (Qiagen) from frozen cell stocks of BL21(D3)pLysS cells containing the pET-14b vector. The plasmid mixture was transformed into Nova Blue cells and grown on LB plates with ampicillin. The controls were cells grown on plates with no drugs and plates with ampicillin and chloramphenicol. A colony from the ampicillin only plate is taken and a 5 mL overnight culture was made. This DNA from the culture was isolated and the procedure was repeated. This was repeated until colonies grow on the ampicillin plate and no drug plate but not the ampicillin and chloramphenicol. When the colony no longer grows on the dual drug plate, then the

colonies on the ampicillin-only plate contained the pET-14b vector and not the pLysS vector.

After the pET-14b vector is purified then the mutagenesis can be performed as described above in chapter 3. The forward primer for H140D is 3'-gat tct att ggc tta gat cga gta gag aac gtc agc c-5' and the reverse primer is 3'-g gct gac gtt ctc tac tcg atc taa gcc aat aga atc-5'.

3.2.2 Characterizing H140D

3.2.2.1 Activity analysis

Assay is conducted as the standard assay described above. 50 μL of H140D CDO is added to an epi-tube to a final concentration of 4.9 μM after the addition of cysteine. 950 μL of Cysteine is also added for a final concentration of 18.7 mM and total volume of 1 mL.

3.2.2.2 Metal analysis

Metal analysis was performed on an ICP-OES. Samples were injected into the nebulizer and analyzed for iron content at the wavelength 238.208 nm. Iron content was then compared to protein concentration to obtain percent iron content.

3.3 Results

H140D was created as the first of three of mutations of the metal binding site that will mimic the 2-his-1-carboxylate motif. This is important because most of the other members of the cupin super family have a 2-his-1-carboxylate motif. The results from this mutation showed that H140D is required for activity and replacing it with an aspartate kills activity. It can be seen in the chromatogram below that H140D lacks the CSA peak (Figure 3.1).

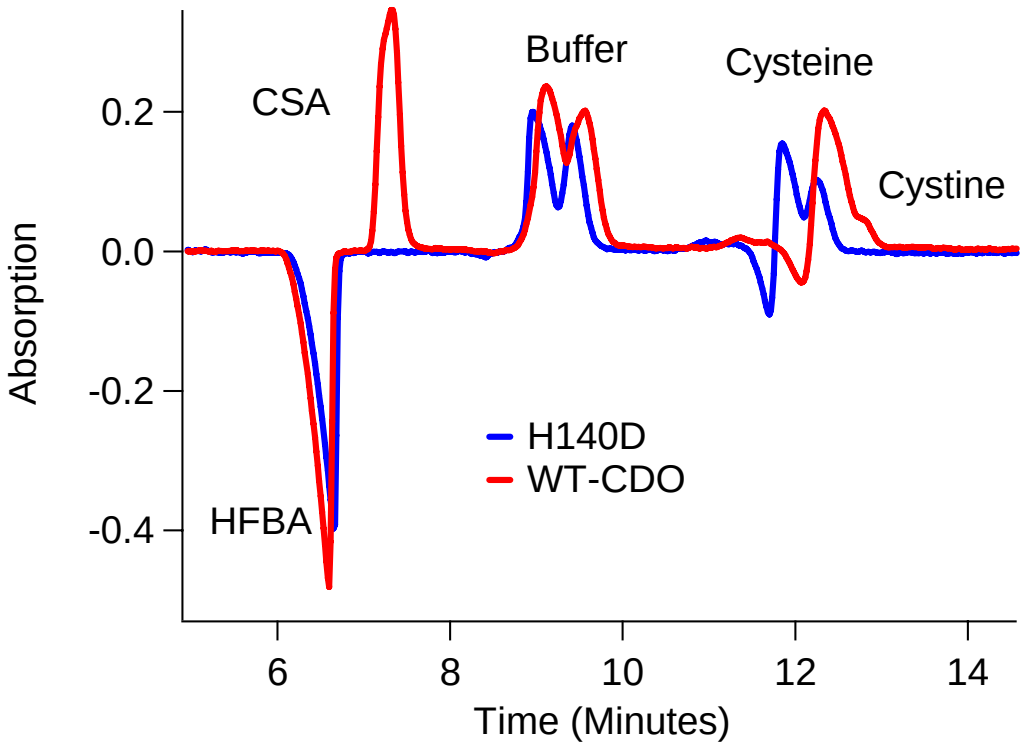

Figure 3.1. HPLC chromatogram with UV detection at 215 nm. The H140D chromatogram clearly shows no CSA peak is present, whereas wild type CDO does have a CSA peak.

3.4 Discussion

To begin the characterization of H140D it was first analyzed for activity. When looking at the HPLC chromatogram it can be easily seen that no CSA is produced under conditions where WT does have product. This peak normally elutes at around 6.5 minutes. If CSA is formed, it is due to the spontaneous oxidation of the thiol of cysteine naturally. This amount of CSA that is naturally formed under these conditions is not detectable. H140D binds approximately 7% ferrous, so it is known that the lack of activity is not caused by the lack of iron incorporation.

Since the mutant was found to be inactive it suggests that CDO may not undergo oxygen activation. The reasoning behind this theory is supported by the fact

that when the carboxylate is introduced into the metal binding center it would add more electron density to the iron. This would cause more oxygen activating potential for the iron. If the mechanism of the CDO reaction goes via oxygen activation then the addition of the carboxylate might increase enzyme activity instead of killing it. Also in nature the thiol of the cysteine substrate becomes oxidized very easily and in fact CSA is formed naturally as mentioned before. Usually the oxidation of the thiol results in a disulfide bond with another cysteine, forming cystine. Since the thiol oxidizes easily, oxygen activation is not necessarily needed to perform the reaction that CDO catalyzes. Thus, CDO is present for a different reason other than activating oxygen for attack on cysteine.

It is possible that since CDO has a unique binding pocket that it also reacts uniquely. Since CDO does not use oxygen activation it is possible that CDO may react via a substrate activating pathway where a sulfur radical develops and attacks the oxygen to form the sulfur-peroxo intermediate.

Next step for characterization of H140D requires a return to Stanford for XAS analysis. Samples have been prepared but yet to be analyzed due to time constraints on the beam line.

3.5 References

(1) Gough J, Karplus K, Hughey R, Chothia C. Assignment of homology to genome sequences using a library of hidden Markov models that represent all proteins of known structure. *J. Mol. Biol.* **2001**, 313, 903-919.

(2) Straganz GD, Nidetzky B. Variations of the 2-his-1-carboxylate them in mononuclear non-heme Fe(II) oxygenases. *Chem. Biochem.* **2006**, 7, 1536-1548.

(3) Hausinger RP. Fe(II)/α-ketoglutarate-dependent hydroxylases and related enzymes. *Critical Reviews in Biochemistry and Molecular Biology*. **2004**, 39, 21-68

(4) Abbott MT, Udenfield S. α-ketoglutarate-coupled dioxygenases, Molecular Mechanisms of Oxygen Activation. *Hayaishi, Ed., Academic Press, New York*. **1974**, 167-214.

CHAPTER 4

XAS STUDIES OF THE METAL BINDING SITE OF CYSTEINE DIOXYGENASE

4.1 Introduction to XAS Techniques

X-ray absorption spectroscopic (XAS) techniques are used to determine the local structure of the metal site. The two specific regions of the XAS spectra that were used in this study were extended x-ray absorption fine structure (EXAFS) and x-ray absorption near edge spectra (XANES). Each spectrum tells a different story. Coordination number and geometry can be determined by XANES analysis of features found below the edge energy. EXAFS is found above the edge and can be used to determine bond lengths and what type of atom the metal is bonded to.

The theory behind XANES involves an x-ray tuned to the absorption energy of the core electron of the element being analyzed. The atom absorbs the x-ray and a core electron is excited. The edge corresponds to the energy at which the electron is ejected. This is referred to as the white line. Pre-edge features correspond to high-energy electron transitions such as a 1s→3d transition. The area of this peak contains information on what the coordination geometry of the target atom maybe.[1]

The EXAFS region begins at about 200eV above the edge. The ejected photoelectron has inherent wave properties that give rise to constructive and destructive interference with photoelectron waves that are backscattered from nearby atoms.[1] Using the equation below it is possible to extrapolate information about the metal center of the enzyme from the EXAFS.[2] Figure 4.1 outlines what information comes from which parts of the EXAFS more simply.[2]

$$\chi(k) = \sum_s \frac{N_s |f_s(\pi,k)|}{kR_{as}^{\ 2}} \exp\left(-R_{as}/\lambda_f\right) \exp\left(-2\sigma_{as}^{\ 2}k^2\right) \sin\left[2kR_{as} + \alpha_{as}(k)\right]$$

Table 4.1 Variables and their meanings to the equation above

Variable	Meaning
N_s	Number of scattering atoms in the shell
$\lvert f_s(\pi,k) \rvert$	Inherent backscattering amplitude for this type of scattering atom
R_{as}	Distance between absorbing atom and the scattering atoms in this shell (Å)
λ_f	Mean free path for inelastic scattering of photo electrons (Å)
$\sigma_{as}^{\ 2}$	The rms deviation of $R_{as}\exp(-2\ \sigma_{as}^{\ 2}k^2)$ is referred to as the Debye-Waller factor
$\alpha_{as}(k)$	The inherent backscattering phase shift for this absorbing/scattering atom combination.

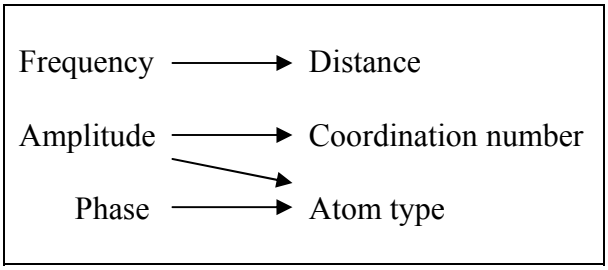

Figure 4.1 Simplified outline of EXAFS features and the information obtained from them.

XAS is typically done at synchrotron sources because a variable x-ray source is needed as well as high intensities. Several are located around the world. The CDO XAS experiments were performed at Stanford University using the SSRL beam-line 9-3.

4.2 Experimental

4.2.1 XAS sample preparation

Sample preparation was done in anaerobic conditions. The thrombin cleaved CDO from the protocol in section 1.2.5 was reconstituted with Fe (II) ammonium sulfate. The CDO is in 50mM HEPES, pH 7.5 and contains 100 mM NaCl. EDTA was added to the sample of CDO and allowed to sit for one hour before being

removed by buffer exchange. Iron was added to a final concentration that was twice that of the concentration of CDO and allowed to sit for 2 hours and then chelexed and buffer exchanged to remove excess iron. The CDO was 217 μM and thus the final concentration of iron during reconstitution was 434 μM. The CDO was then concentrated to 500 μM.

30 μL of the CDO is aliquoted into an epi-tube with 1 μL of a 62 mM solution of cysteine for a final concentration of 2 mM cysteine. Another sample prepared with just the activator, cysteamine, was made the same way but with a 62 mM solution of cysteamine. A control sample was also made without substrate or activator. Sample analysis was performed at Stanford University at the SSRL beam line 9-3. Other iron samples that were made for a second trip to the beam line include the mutant H140D and H140D with cysteine. These samples were prepared using cleaved H140D CDO and used the same procedures as above except using mutant cleaved CDO instead. Some nickel samples were also prepared by using nickel chloride in place of the ferrous ammonium sulfate during metal reconstitution. These samples include Ni-CDO and Ni-CDO with cysteine. Metal content was determined after samples were analyzed by XAS. This is done on the ICP-OES

4.2.2 XAS analysis methods

Sample analysis was performed at Stanford University at the SSRL beam line 9-3. Analysis was done at 10 K using a liquid helium cryostat. The ring conditions were 3 GeV and 80-100 mA. The optics consisted of a Si(220) double-crystal monochromator and two rhodium coated mirrors. A flat mirror before the monochromator was used for harmonic rejection and vertical collimation, and a

toroidal mirror after the monochromator was for focusing. The detector at this beamline was a 30-element germanium detector (Canberra). A set of soller slits with a Z-1 element filter was placed between the sample chamber and detector to minimize scattering. XANES was collected from ±200 eV relative to the edge. EXAFS was collected from 13.5-16 K above the edge energy.[3]

4.3 Results

The EXAFS that was obtained from the beam trip did not have good enough signal to noise ratio for analysis due to low metalated CDO concentration. However, there was some useful data obtained from the XANES spectra. It can be seen that the sample that contained the activator cysteamine was very different than the CDO sample and the CDO with substrate sample. The differences can be seen in the 1s → 3d transition peak area as well as the white line intensity at approximately 7135 eV (figure 4.2).

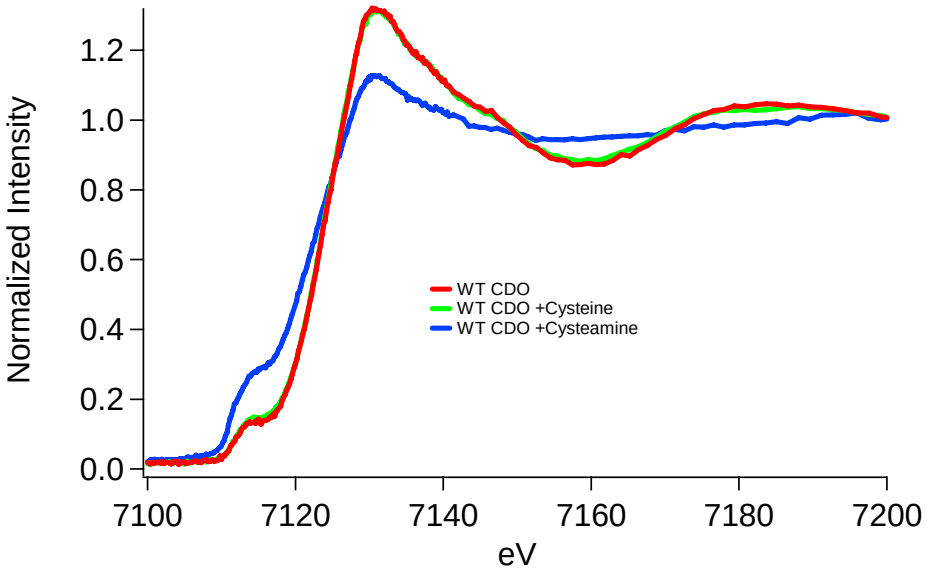

Figure 4.2 XANES spectra clearly showing large differences in 1s → 3d and edge peak intensities.

To ensure that metal concentrations are high enough for analysis by XAS, metal analysis was done on the samples post analysis. The metal content of the samples that were analyzed were all 12% of enzyme had iron bound. This means that the iron concentration was approximately 60 μM because the protein was 500 μM. Metal analysis on samples that were not analyzed by XAS was not performed yet. There is a limited amount of protein when making samples due to low protein expression and slow protein cleavage thus all protein that is cleaved is used to make samples. Only after the samples are analyzed by XAS then can be used to determine metal analysis because samples are not retrievable after analysis with ICP-OES.

4.4 Discussion

To further elucidate the coordination number and binding geometry of the metal binding site of CDO, the power of x-ray absorption spectroscopy was used. The purpose of the technique was to determine the geometry of the binding site, what ligands bind the iron center, and their distances from the iron. When looking at the results for the three samples that were analyzed it can be seen easily that the cysteamine XANES is quite different than the other two. The enzyme and the enzyme/substrate complex look very similar which confers with prior results obtained previously. Also it was previously found that the substrate does not bind by the thiol. It is suggested that the substrate may not bind to the iron at all, which is supported by the results since there is so little change in the XANES spectra.

Unfortunately no conclusive data can be determined from the EXAFS of the three samples. There was a great amount of noise past 3.5 Å and it is unclear what peaks were noise and what may be data. Previous experiments by a former student

showed similar XANES spectra and the EXAFS from these showed six N/O ligands on samples of CDO without cysteine and CDO with cysteine (figure 4.3)[4].

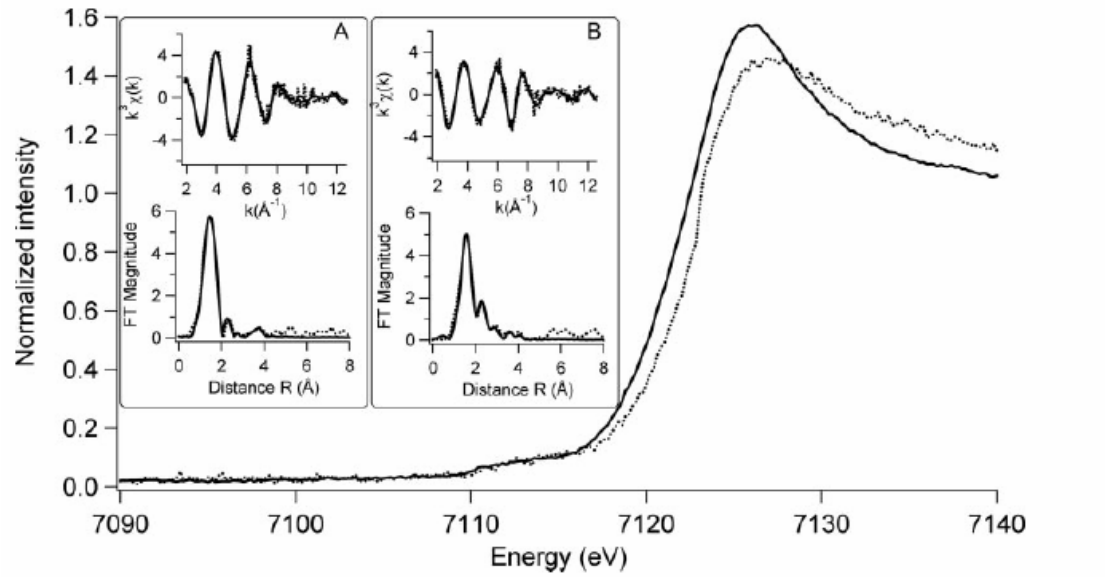

Figure 4.3. EXAFS and XANES of CDO without cysteine (A, solid line) and with cysteine (B, dotted line) showing a white line around 7128 eV. The Fourier transform show 6 N/O donors on both samples.[4]

More samples of for XAS analysis were made but due to time constraints they were not analyzed. The unique mutant H140D was made to probe the metal binding site and to see if there is a change in binding coordination from wild-type CDO. H140D is the first of a series of mutants made to mimic the 2-histidine-1-carboxylate motif that most other members of the cupin superfamily of oxygenases. This motif is interesting because most other members with this motif also require α-ketoglutarate where it acts as a reducing agent. Also these enzymes with the 2-histidine-1-carboxylate motif undergo oxygen activation. Nickel samples were also made and not analyzed. These include nickelated CDO and nickelated CDO with cysteine bound. The purposes of these were to see if nickel changes the coordination number and

geometry of the metal binding site. Also to see if there are any changes in the way the substrate may bind to this alternate although non-active metal.

4.5 References

(1) Gurman SJ. Interpretation of EXAFS Data. *J. Synchro. Rad.* **1995**, 2, 56-63.

(2) Scott RA, Que L. Physical methods in bioinorganic chemistry: spectroscopy and magnetism. *University Science Books*. **2000**, 465-475.

(3) Leitch S, Bradley MJ, Rowe JL, Chivers PT, Maroney MJ. Nickel-specific response in the transcriptional regulator, *Escherichia coli* NikR. *J. Am. Chem. Soc.* **2007**, 129(16), 5085-5095.

(4) Chai SC, Bruyere JR, Maroney MJ. Probes of the catalytic site of cysteine dioxygenase. *J. Biol. Chem.* **2006**, 238(23), 15774-15779.

CHAPTER 5

CDO ACTIVITY INHIBITORS REVISISTED

5.1 Introduction

Sergio Chai, a former student of the lab, tested several compounds to see their effect on CDO activity. Some of these compounds were found to be inhibitors of CDO. These included homocysteine, mercaptopropionic acid, aspartic acid, α-ketoglutarate, and S-carboxymethyl-cysteine.[1] The common factor between these compounds is that they are structural analogs of cysteine and also contain a negatively charged side chain.[1] Other compounds were tested that did not have negative side chains and were not found to be inhibitors.[1]

CDO was the first non-heme iron dioxygenase that was discovered to be inhibited by α-ketoglutarate. In fact other non-heme iron dioxygenases use α-ketoglutarate as a co-substrate.[2] These oxygenases are known as intermolecular dioxygenases where one oxygen atom is inserted into the substrate and the other oxygen is added to the α-ketoglutarate.[2] It is clear that CDO is not an intermolecular dioxygenase because it utilizes both oxygen atoms in its reaction.

In this chapter we will be revisiting the inhibitors that were tested previously. It was found that aspartate in particular inhibited CDO by about 50%. The previous inhibition experiments were conducted in phosphate buffer (50 mM phosphate pH 7.5, 100 mM NaCl). Also as well as phosphate, ammonium acetate solution (50 mM ammonium acetate, pH 7.5, 100 mM NaCl) was also used for other experiments. As mentioned before, experiments have changed to be conducted in HEPES buffer (50 mM Hepes, pH 7.5, 100 mM NaCl) due to solubility problems when using phosphate

buffer. Phosphate salts are insoluble when they form the compounds ferrous phosphate and calcium phosphate.

Retesting of aspartate as an inhibitor was needed to determine what class of inhibitor it was. This experiment was conducted in HEPES buffer instead of phosphate buffer and a surprising result occurred. Aspartate caused an increase in CDO activity instead of inhibiting it. These results stimulated new experiments to elucidate why aspartate acts as an inhibitor in phosphate buffer but an activator in HEPES buffer.

5.2 Experimental

5.2.1 Aspartate inhibition assay

This was an assay to determine what type of inhibitor aspartate was. The assay conditions used HEPES buffer (50 mM HEPES, pH 7.5, 100 mM NaCl). The controls had no inhibitor added to the reactions. 50 μL of 62 μM CDO was diluted with HEPES buffer with cysteine. The cysteine concentration varied from 0 mM to 13.9 mM over eight reactions. There were two tests done, one with aspartate as the inhibitor and one with acetate as another inhibitor. These tests had the same CDO and cysteine concentrations but also added were the inhibitors to their respective reactions to a final concentration of 9 mM. Reactions were incubated for about 3 hours and 50 minutes. Assays were analyzed on the HPLC as the protocol stated above in section 1.2.3.1.

5.2.2 Buffer inhibition assay

CDO was buffer exchanged into phosphate buffer, ammonium acetate solution, and HEPES buffer. Two 50 μL aliquots per buffer were added to epi-tubes

totaling six samples. The samples were reacted and analyzed as stated in the activity assay protocol above (Section 1.2.4.1) except that aspartate is also added to one of the tubes per buffer at a final concentration of 2mM.

5.2.3 Metal chelation by aspartate

CDO at a concentration of 200 μM was taken and aliquoted into three 6 mL volumes. These were buffer exchanged into the three different solutions. The solutions were phosphate buffer, ammonium acetate solution, and HEPES buffer. Each of these buffers was 50 mM, pH 7.5 and also contained 100mM NaCl. They were buffer exchanged and concentrated using 10,000 Da spin concentrators down to a final volume of 2 mL. After buffer exchanging the three samples were each split into two aliquots and added to epi-tubes. To one aliquot of each buffer sample, aspartic acid was added to a final concentration of 2 mM. These were incubated for 15 minutes at room temperature. The six samples were then buffer exchanged into their respective buffers to remove any aspartic acid and unbound metal. The samples were then analyzed for iron content on an ICP-OES.

5.2.4 Retesting of previously found inhibitors in HEPES buffer

A selection of the previously investigated inhibitors were experimented in HEPES buffer. The compounds selected were homocysteine, α-ketoglutarate, and S-carboxymethyl-cysteine. The reaction conditions 500 μL of 30 mM cysteine and 450 μL of 30 mM inhibitor were added to 50 μL of CDO. The assay conditions were the same as previously said above by incubation in 37 ^{o}C water bath for 4 hours.

5.3 Results

A number of different buffers were used through out the experiments during the studying of CDO by the current student as well as previous students. The three solutions were phosphate, ammonium acetate solution, and HEPES. All of them were pH 7.5 and also contained 100mM NaCl. The effect of the buffer was put into question when it was found that in HEPES, aspartic acid acted as an activator. This was odd because it was previously found previously that aspartic acid was an inhibitor.[1] The experiments that found that aspartic acid was an inhibitor utilized the phosphate buffer.

The aspartate inhibition assay was conducted to determine what type of inhibitor it was. The results of the assay concluded that aspartate was in fact an activator instead of inhibitor. Aspartate at high concentrations of cysteine increased activity by approximately 8% compared to wild type CDO without aspartate. The acetate portion of this assay inhibited CDO by approximately 40%.

When assays were conducted in the various buffers stated above it was found that in HEPES aspartic acid actually acts as a slight activator. It increased activity by 8%. In phosphate and ammonium acetate solution aspartic acid was found to be an inhibitor. Aspartic acid inhibited activity by 18% and 63% in phosphate buffer and ammonium acetate solution respectively. It was thought that aspartate may be chelating the iron and extracting it out of CDO. The results from the metal analysis from the chelating experiment found that the samples of CDO in HEPES buffer contained 14.9% iron and 15.9% with aspartate. CDO in phosphate buffer and ammonium acetate solution had a decrease in iron content when aspartate was added

from 14.5% to 12.3% and 14.3% to 7.0%. This correlates to an increase in iron in HEPES buffer by 6.7% and a decrease by phosphate buffer and ammonium acetate solution by 15.1% and 51.0% respectively.

Several compounds that were previously found to be inhibitors were retested in HEPES buffer. The various compounds tested and found to be inhibitors were homocysteine, mercaptopropionic acid, aspartic acid, α-ketoglutarate, and S-carboxymethyl-cysteine. These inhibition assays were performed in phosphate buffer. In the retest it was found that homocysteine, S-carboxymethyl-cysteine, and α-ketoglutarate had an increase in activity by 26.1%, 43.4%, 44.2% respectively when compared to wild type CDO with just cysteine present. The rates and their percent activities compared to wild type CDO with no activator/inhibitor added can be seen in table 5.1. Cysteamine caused no appreciable increase or decrease in activity.

Table 5.1. Activity increases exhibited by CDO with various activators in HEPES buffer, pH 7.5

Retested activators/inhibitors	Rates (mol CSA/min)	Percent activity (Compared to Wild type)
No activator/inhibitor	38.2±7.2	100%
Homocysteine	48.2±6.5	126.1%
S-carboxymethyl-cysteine	54.8±9.3	143.4%
α-ketoglutarate	55.1±8.6	144.2%

5.4 Discussion

In the past it was determined that structural analogs of cysteine with a negative side chain had the ability to inhibit CDO activity. In various tests that were conducted recently it appears that these analogs may not be inhibitors. In fact they activated CDO. A reexamination of the inhibitor aspartate was performed to determine what type of inhibitor it was. These experiments revealed that aspartate is

an activator in the HEPES buffer, pH 7.5. Then another test, the buffer inhibition test, confirmed that aspartate is an activator in HEPES, but it is also an inhibitor in phosphate buffer and ammonium acetate solution.

At first this was confusing because there weren't many indications of what could be happening chemically. Then it was thought that aspartate could be chelating the metal and facilitating removal from the enzyme. After the metal is pulled out the phosphate or acetate can bind to it and keep it from loading back into the enzyme. The negative charges on the ions have the ability to ligate the metal.

To test this theory the aspartate chelating experiment was done. The enzyme was incubated with aspartate in phosphate buffer to rip out the metal and then buffer exchanged for metal analysis. This was compared to enzyme that was not subjected to aspartate. The findings support that aspartate may be facilitating iron removal and then the ligation by phosphate keeps it from reentering the binding site.

As stated above in the results section it was found that the addition of aspartate to HEPES buffer increased the iron content from 14.9% to 15.9%. In the other two buffers the aspartate caused a drop in iron from 14.5% to 12.3% and 14.3% to 7.0% in the phosphate and acetate buffers respectively. This correlated to an increase in iron in HEPES buffer by 6.7% and a decrease by phosphate and acetate buffers by 15.1% and 51.0% respectively. These percentages are very similar to that of the changes in activity. In HEPES buffer the aspartate caused an increase of 8% and a decrease of 18% and 63% in phosphate and acetate respectively. These results support the hypothesis that aspartate aids in iron removal from CDO in phosphate and acetate buffers illustrated in figure 5.1. Thus, when the samples were buffer

exchanged the metal bound to aspartate and the ion could be washed out lowering the amount of metal in solution. In the case of phosphate it is possible that the metal was also removed via precipitation due to the insolubility of iron (II) phosphate.

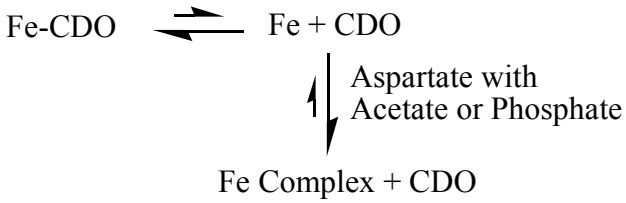

Figure 5.1 Iron equilibrium when aspartate is introduced into reaction.

Metal loading of the enzyme was previously done in ammonium acetate buffer because iron (II) phosphate would form in the phosphate buffer and it is insoluble, but because ammonium acetate is not truly a buffer at pH 7.5 it was still not preferred. Thus, HEPES buffer is currently used to load the enzyme with iron.

Then there is the question of whether the other previously found inhibitors were in fact still inhibitors in HEPES buffer. Thus, the purpose of the retesting was to determine if the inhibitors found previously are infact still inhibitors in the HEPES buffer. These compounds are structural analogs of cysteine and also contain a negative side chain. It was found that structural analogs without the negative side chain had no affect on CDO activity. In the retesting it was found that the structural analogs that were once inhibitors actually had activating qualities in the HEPES buffer. α-ketoglutarate had the largest increase in activity but S-carboxymethyl-cysteine follows closely behind by about one percent.

The activation of CDO by these cysteine analogs gives clues into how the reaction mechanism occurs. One hypothesis is that multiple cysteine molecules maybe bound in the active center and the cysteine that is actually converted to CSA

may not be bound directly to the iron. One cysteine is bound to the iron and the cysteine that is reacted with oxygen is apart of a hydrogen-bonding network with various residues and the cysteine bound to the iron. The activating compounds with the negative side chains may be able to find its way into the active site and bind to the iron more tightly than cysteine. Thus the reaction can occur more quickly when these activators are present.

5.5 References

(1) Chai SC, Bruyere JR, Maroney MJ. Probes of the catalytic site of cysteine dioxygenase. *J. Biol. Chem.* **2006**, 238(23), 15774-15779.

(2) Hausinger RP. Fe(II)/α-ketoglutarate-dependent hydroxylases and related enzymes. *Crit. Reviews in Biochem. And Mol. Biol.* **2004**, 39, 21-68.

BIBLIOGRAPHY

Abbott MT, Udenfield S. α-ketoglutarate-coupled dioxygenases, Molecular Mechanisms of Oxygen Activation. *Hayaishi, Ed., Academic Press, New York*. **1974**, 167-214.

Chai SC, Bruyere JR, Maroney MJ. Probes of the catalytic site of cysteine dioxygenase. *J. Biol. Chem.* **2006**, 238(23), 15774-15779.

Chai SC, Jerkins AA, Banik JJ, Shalev I, Pinkham JL, Uden PC, Maroney MJ. Heterologous expression, purification, and characterization of recombinant rat cysteine dioxygenase. *J. Biol. Chem.* **2005**, 280(11), 9865-9869.

Chen LY, Doi N, Durley RCE, Chistoserdov AY, Lidstrom ME, Davidson VL, Mathews FS. Refined crystal structure of methylamine dehydrogenase from *Paracoccus denitrificans* at 1.75 Å resolution. *J. Mol. Biol.* **1998**, 276, 131-149.

Dominy JE Jr., Hwang J, Stipanuk MH. Overexpression of cysteine dioxygenase reduces intracellular cysteine and glutathione pools in HepG2/C3A cells. *Am J Physiol Endocrinol Metab* **2007**, 293(1), E62-E69.

Dunwell JM, Culham A, Carter CE, Sosa-Aguirre CR and Goodenough PW. Evolution of functional diversity in the cupin superfamily. *Trends Biochem. Sci.* **2001**, 26, 740-746

Emery P, Bradley H, Gough A, Arthur V, Jubb R, Waring R. Increased prevelance of poor sulfoxidation in patients with rheumatoid-arthritis – effects of changes in the acute phase response and 2nd-line drug-treatment. *Annals of the Rheumatic Diseases* **1992**, 51, 318-320.

Firbank SJ, Rogers MS, Wilmot CM, Dooley DM, Halcrow MA, Knowles PF, McPherson MJ, Phillips SEV. Crystal structure of the precursor of galactose oxidase: An unusual self-processing enzyme. *PNAS***. 2001**, 98(23), 12932-12937.

Gough J, Karplus K, Hughey R, Chothia C. Assignment of homology to genome sequences using a library of hidden Markov models that represent all proteins of known structure. *J. Mol. Biol.* **2001**, 313, 903-919.

Griffith OW. *Mammalian sulfur amino acid metabolism*. Academic Press: Orlando, Florida, **1987**, 143

Guionrain MC, Portemer C, Chatagner F. Rat-liver cysteine sulfinate decarboxylase – purification, new appraisal of molecular-weight and determination of catalytic properties. *Biochimica Et Biophysica Acta* **1975**, 384, 265-276.

Gurman SJ. Interpretation of EXAFS Data. *J. Synchro. Rad.* **1995**, 2, 56-63.

Hausinger RP. Fe(II)/α-ketoglutarate-dependent hydroxylases and related enzymes. *Critical Reviews in Biochemistry and Molecular Biology*. **2004**, 39, 21-68

Hirschberger LL, Daval S, Stover PJ, Stipanuk MH. Murine cysteine dioxygenase gene: structural organization, tissue-specific expression and promoter identification. *Gene* **2001**, 277, 153-161.

Janes SM, Mu D, Wemmer D, Smith AJ, Kaur S, Maltby D, Burlingame AL, Klinman JP. A new redox cofactor in eukaryotic enzymes: 6-hydroxydopa at the active site of bovine serum amine oxidase. *Science*. 1990, 248, 981-987.

Kalatzis V, Antignac C. Cystinosis: from gene to disease. *Nephrology Dialysis Transplantation* **2002**, 17, 1883-1886.

Kalatzis V, Cherqui S, Antignac C, Gasnier B. Cystinosin, the protein defective in cystinosis, is a H+-driven lysosomal cystine transporter. *EMBO Journal* **2001**, 20, 5940-5949.

Klabunde T, Eicken C, Sacchettini JC, Krebs B. Crystal structure of a plant catechol oxidase containing a dicopper center. *Nat. Struct. Biol.* **1998**, 5, 1084-1090.

Laemmli UK. Cleavage of structural proteins during the assembly of the head of bacteriophage T4. *Nature*. **1970**, 227(5259), 680-685.

Leitch S, Bradley MJ, Rowe JL, Chivers PT, Maroney MJ. Nickel-specific response in the transcriptional regulator, *Escherichia coli* NikR. *J. Am. Chem. Soc.* **2007**, 129(16), 5085-5095.

McCoy JG, Bailey LJ, Bitto E, Bingman CA, Aceti DJ, Fox BG, Phillips GN. Structure and mechanism of mouse cysteine dioxygenase. *P. Natl. Acad. Sci. USA*. **2006**, 103, 3084-3089.

Okeley NM, Van der Donk WA. Novel cofactors via post-translational modifications of enzyme active sites. *Chem. Biol.* 7, R159-R171.

Ostermeier C, Harrenga A, Ermler U, Michel H. Structure at 2.7 Å resolution of the *Paracoccus denitrificans* two-subunit cytochrome *c* oxidase complexed with an antibody Fv fragment. *Proc. Natl. Acad. Sci. USA*, **1997**, 94, 10547-10553.

Parsons RB, Ramsden DB, Waring RH, Barber PC, Williams AC. Hepatic localisation of rat cysteine dioxygenase. *J. Hepatol*. **1998**, 29, 595-602.

Parsons RB, Waring RH, Ramsden DB, Williams AC. In vitro effect of the cysteine metabolites homocysteic acid, homocysteine and cysteic acid upon human neuronal cell lines. *Neurotoxicology* **1998**, 19, 599-603.

Perry TL, Norman MG, Yong VW, Whiting S, Crichton JU, Hansen S, Kish SJ. Hallervorden-Spatz disease – cysteine accumulation and cystine dioxygenase deficiency in *Globus pallidus*. *Annals of Neurology* **1985**, 18, 482-489

Scott RA, Que L. Physical methods in bioinorganic chemistry: spectroscopy and magnetism. *University Science Books*. **2000**, 465-475.

Simmons CR, Karplus PA, Stipanuk MH. 1.5 A Resolution R. Norvegicus Cysteine Dioxygenase Structure Crystallized in the Presence of Cysteine. Unpublished but PDB deposited.

Simmons CR, Liu Q, Huang Q, Hao Q, Begley TP, Karplus PA, Stipanuk MH. *J. Biol. Chem.* **2006**, 281, 18723-18733.

Singer TP, Kearny EB. Intermediary metabolism of L-cysteinesulfinic acid in animal tissues. *Archives of Biochemistry and Biophysics* **1956**, 61, 397-409.

Stipanuk MH, Londono MP, Lee JI, Hu M, Yu AF. Enzymes and metabolites of cysteine metabolism in nonhepatic tissues of rats show little response to changes in dietary protein or sulfur amino acid levels. *J. Nutr* **2002**, 132, 3369-3378.

Straganz GD, Nidetzky B. Variations of the 2-his-1-carboxylate them in mononuclear non-heme Fe(II) oxygenases. *Chem. Biochem.* **2006**, 7, 1536-1548.

Tsuboyama N, Hosokawa Y, Totani M, Oka J, Matsumoto A, et al. Structural organization and tissue-specific expression of the gene encoding rat cysteine dioxygenase. *Gene* **1996**, 181, 161-165

Whittaker MM, Duncan WR, Whittaker JW. Synthesis, structure, and properties of a model of galactose oxidase. *Inorganic Chem.* **1996**, 35, 382-386.

Whittaker MM, Kerstern PJ, Nakamura N, Sanders-Loehr J, Schweizer ES, Whittaker JW. Crystal structure of the precursor of galactose oxidase: An unusual self-processing enzyme. *J. Biol. Chem.* **271**, 681-687.

Wilkinson LJ, Waring RH. Cysteine dioxygenase: modulation of expression in human cell lines by cytokines and control of sulphate production. *Toxicol. In Vitro*. **2002**, 16, 481-483.

Ye S, Wu X, Wei L, Tang D, Sun P, Bartlam M, Rao Z. Insight into the mechanism of human cysteine dioxygenase key roles of the thioether-bonded-tyrosine-cysteine cofactor. *J. Biol. Chem.* **2007**, 282(5), 3391-3402.